Geomechanics and Engineering, *Vol. 29, No. 3 (2022) 281-290*
https://doi.org/10.12989/gae.2022.29.3.281

Experimental study for application of the punch shear test to estimate adfreezing strength of frozen soil-structure interface

Sangyeong Park[1a], Chaemin Hwang[1b], Hangseok Choi[1c], Youngjin Son[2d] and Tae Young Ko*[3]

[1]*School of Civil, Environmental and Architectural Engineering, Korea University, 145, Anam-ro, Seongbuk-gu, Seoul, Korea*
[2]*Eco Infra Solution Team, SK ecoplant, 32 Insadong 7-gil, Jongno-gu, Seoul, Korea*
[3]*Department of Energy and Resources Engineering, Kangwon National University, 1, Kangwondaehak-gil, Chuncheon-si, Gangwon-do, Korea*

(Received January 20, 2022, Revised March 3, 2022, Accepted March 10, 2022)

Abstract. The direct shear test is commonly used to evaluate the shear behavior of frozen soil-structure interfaces under normal stress. However, failure criteria, such as the Mohr–Coulomb failure criterion, are needed to obtain the unconfined shear strength. Hence, the punch shear test, which is usually used to estimate the shear strength of rocks without confinement, was examined in this study to directly determine the adfreezing strength. It is measured as the shear strength of the frozen soil-structure interface under unconfined conditions. Different soils of silica sand, field sand, and field clay were prepared inside the steel and concrete ring structures. Soil and ring structures were frozen at the target temperature for more than 24 h. A punch shear test was then conducted. The test results show that the adfreezing strength increased with a decrease in the target temperature and increase in the initial water content, owing to the increase in ice content. The adfreezing strength of field clay was the smallest when compared with the other soil specimens because of the large amount of unfrozen water content. The field sand with the larger normalized roughness showed greater adfreezing strength than the silica sand with a lower normalized roughness. From the experiment and analysis, the applicability of the punch shear test was examined to measure the adfreezing strength of the frozen soil-structure interface. To find a proper sample dimension, supplementary experiments or numerical analysis will be needed in further research.

Keywords: adfreezing strength; frozen soil-structure interface; ice content; punch shear test; unfrozen water content

1. Introduction

Frozen soils show different behavior from unfrozen soils in terms of thermal-mechanical-hydraulic properties, due to ice (Zhou *et al.* 2018, Zhang *et al.* 2019, Jin *et al.* 2020, Wang *et al.* 2020). Thus, various researchers have investigated the effect of the existence of ice on the behavior of frozen soil. Burt and Williams (1976) measured the hydraulic conductivity of multiple frozen soils and discovered that the hydraulic conductivity was dependent on the temperature due to the phase change. Sayles and Carbee (1981) showed that the maximum unconfined compressive strength of frozen silt increased as the ice content increased. Arenson *et al.* (2004) found that the behavior of frozen soil is highly related to volumetric ice content and strain rate. Thomas *et al.* (2009) used the hydraulic permeability coefficient as a function of temperature and constructed a heat transfer equation considering ice.

Additionally, the frozen soil can adhere to the surface of underground structures, such as pile foundations, retaining walls, or shield tunnel segments via ice. This process is called adfreezing, and the adfreezing strength is defined as the maximum shear stress that causes the interface between the frozen soil and the surface of the structures to slip. Adfreezing strength, which contributes to resisting the downward load, is an essential factor for calculating the bearing capacity of pile foundations in frozen ground (Parameswaran 1978, Weaver and Morgenstern 1981, He *et al.* 2020). Whereas, when the ground freezing method was applied in the shield TBM construction, adfreezing itself can damage the tunnel segment or provide an additional load to the shield machine to obstruct the construction process (Quanbin *et al.* 2018). The adfreezing strength is affected by diverse factors, such as temperature, soil properties, water content, material of structure, rate of load application, and confining stress. Therefore, estimating the adfreezing strength under various conditions is necessary for construction work in frozen soil (Wand *et al.* 2018, Wang *et al.* 2020).

Many studies have explored the adfreezing strength through direct shear tests under different conditions (Ko and Choi 2011, Choi 2011, Lee *et al.* 2013, Tang *et al.* 2020,

*Corresponding author, Assistant Professor
E-mail: tyko@kangwon.ac.kr
[a]Ph.D. student
E-mail: kjk00095@korea.ac.kr
[b]M.S. student
E-mail: hcm5536@korea.ac.kr
[c]Professor
E-mail: hchoi2@korea.ac.kr
[d]General Manager, Ph.D.
E-mail: sohnyjin@daum.net

ISSN: 2005-307X (Print), 2092-6219 (Online)

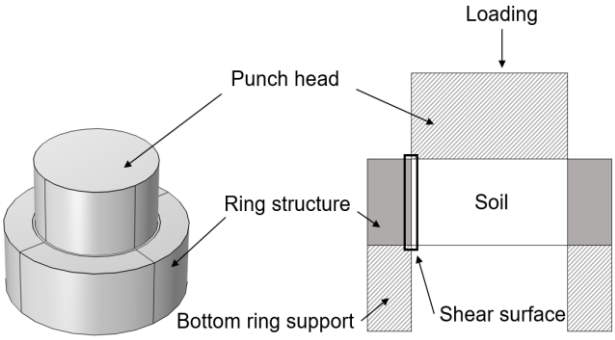

Fig. 1 Schematics of punch shear test setup and shear surface

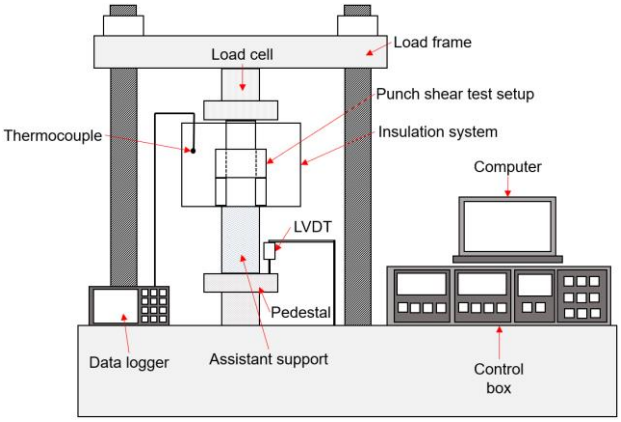

Fig. 2 Compression apparatus

Peng-Fei *et al*. 2021). Liu *et al.* (2014) performed large-scale direct shear tests using remolded silty clay and concrete. They showed the shear stress-displacement curves under various testing conditions such as normal pressure, temperature, and water content. Wang *et al.* (2019) suggested a roughness algorithm for the normalized roughness index of the soil-structure interface. They found that the shear strength showed a positive linear relationship with the roughness under different values of normal pressure, temperature, and initial water content in the direct shear test.

The abovementioned studies discovered that the peak shear strength, similar to the concept of adfreezing strength, increased with decreasing temperature and showed a proportional relationship with normal stress and initial water content. Although the direct shear test can consider the effect of normal stress and is easy to make a specimen, failure models should be used to gain shear strength with zero normal stress, which is the minimum shear strength, such as the Mohr-Coulomb criterion (Ladanyi 1995). Hence, a new experimental method is required to directly assess the unconfined adfreezing strength. This adfreezing strength can be used for the conservative design of pile foundation.

Terashima (1997) summarized four conceptual experiments to evaluate adfreezing strength: push-out, pull-out, twist, and shear tests, and concluded that the four tests showed the same results. The purpose of this study is to examine the applicability of the punch shear test, a type of push-out test, to evaluate the adfreezing strength, depending on soil type, materials of structure, temperature, and water content. In rock mechanics, the shear strength of rock with zero confinement could be obtained through the punch shear test (Jaeger 1979, Li *et al.* 2017, Wu *et al.* 2017, Xu *et al.* 2019). Based on this knowledge, the punch shear was introduced to determine the maximum shear stress, which had the frozen soil detached from the ring structure, by developing a new method for specimen preparation. The test results were analyzed with the unfrozen water content calculated using empirical approaches.

2. Experimental work

2.1 Punch shear test and test apparatus

The punch shear test is a common test method for measuring the shear strength of thin disc rock specimens. Shear stress is delivered by a compressive force through a cylindrical punch head parallel to the shear surface (Zhu and Li 2021). To apply the punch shear test for adfreezing estimation, a suitable specimen preparation method was developed with a ring structure. As shown in Fig. 1, the punch test consisted of a punch head, a soil-ring structure, and a bottom ring support. The punch head, whose diameter was equal to the inner diameter of the ring structure, carried a normal load on the soil-ring structure. The soil-ring structure held out the compressive force on its shear surface, where the soil specimen met the ring structure and was then separated into soil specimens and ring structures if the shear stress exceeded the adfreezing strength. The bottom ring support propped up only the ring structure so that the soil specimen could be slipped down alone.

Table 1 The basic physical properties of soils

	Specific gravity (Gs)	Coefficient of uniformity (Cu)	Coefficient of Curvature (Cc)	Liquid limit (LL), [%]	Plastic limit (PL), [%]	Classification (USCS)
Silica sand	2.65	0.02	0.87	NP	NP	SP
Field sand	2.66	2.27	1.18	NP	NP	SP
Field clay	2.72	-	-	61.98	30.93	CH

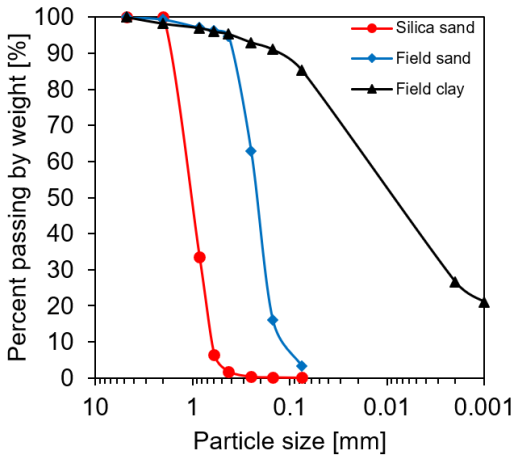

Fig. 3 Particle size distribution curves of the test soil

(a) Stainless steel ring structure

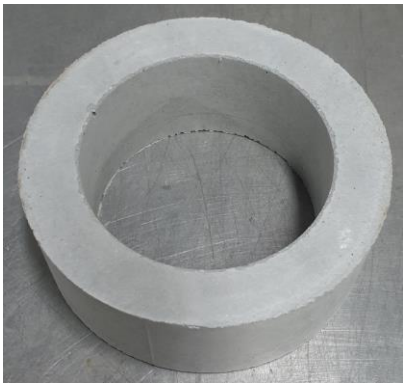

(b) Concrete ring structure

Fig. 4 Ring structure

The adfreezing strength σ_{adf} can be calculated using Eq. (1) as the maximum value of the compressive force divided by the shear surface area.

$$\sigma_{adf} = \frac{F_{max}}{\pi DH} \tag{1}$$

where F_{max} is the maximum value of the compressive force, D is the inner diameter of the ring structure, and H is the height of the ring structure.

The compression apparatus shown in Fig. 2 was utilized to employ a compressive force on the punch head for the punch shear test. This apparatus includes a servomotor and frame that applies a load, a control box that can directly control the servomotor, a computer that records the load displacement of the sample and adjusts the deformation rate during the test, and a thermocouple and data logger that can measure the temperature inside the insulation system to maintain a constant temperature of the punch shear test setup. A load cell was installed on the upper part of the main body, and a cylindrical assistant support to hold up the insulation system was located in the center. The servomotor located at the bottom raises the pedestal upward and applies a load to the punch head. The displacement of the sample was measured using an LVDT installed on the pedestal.

2.2 Soil specimens and ring material

Silica sand, field sand, and field clay were prepared as the soil specimens. Field sand and field clay were taken from the downstream area of the Nakdong River Delta, Korea. The basic physical properties of the soil are listed in Table 1, and the particle size distribution curves are shown in Fig. 3.

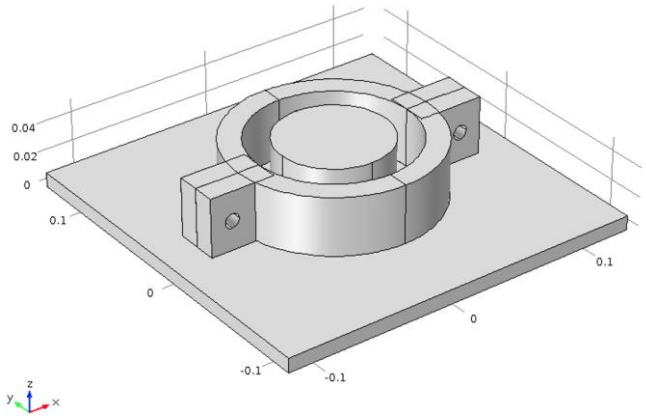

(a) Schematics of Teflon mold

(b) Overview of Teflon mold

Fig. 5 Teflon mold for concrete ring structure preparation

The materials of the ring structures were stainless steel and concrete (Fig. 4). And the concrete consisted of ordinary Portland cement and water, at a mixing ratio of 100:14. A Teflon mold was specially designed for manufacturing the concrete ring structure. As shown in Fig. 5, the Teflon mold included a base plate, two external units, and a central cylinder unit. Two external units and the central cylinder unit can be fixed on the base plate by bolting. Also, the external units were assembled with bolts and nuts, which made it easy to take out the cured concrete ring structure.

The inner diameter of the ring structure was 76 mm, the outer diameter was 110 mm, and the height was 40 mm. The punch head and bottom ring supports were made of stainless steel. The diameter of the punch head and inner diameter of the bottom ring support were equal to the inner diameter of the ring structure (76 mm). In addition, the heights of the punch head and bottom ring support were 40 mm.

2.3 Test method

A mold for soil-ring structure preparation is illustrated in Fig. 6. The mold was made of stainless steel to guarantee high rigidity and thermal conductivity. The mold consisted of a back mold unit, a front mold unit, and porous upper and lower plates. The back and front mold units were assembled by bolting at each side, and a rubber packing was installed between the mold units for waterproofing. A valve was connected to the front mold unit to supply water into the soil sample. Two bolts were installed between the four assembly bolts to push the back mold unit from the front mold unit after freezing, making it easy to separate. The lower porous plate was designed to have the same diameter as the inner diameter of the ring, which is identical to the diameter of the soil sample. The upper porous plate was designed to have the same diameter as the outer diameter of the ring. In addition, a rod was installed on the upper porous plate to hold weights to press evenly the frozen soil sample. During the soil-ring sample preparation in the saturated conditions, the filter paper was placed between the porous plates to hold soil particles with free water drainage. In contrast, the impermeable plastic wrap was used instead of the filter paper to maintain the target initial water content in the unsaturated conditions.

Soil-ring structures were fabricated in the mold by compacting soil specimens inside the ring structures and then frozen together at the target temperature. The target temperature was designed as -5, -10, -15, and -20°C. The initial water content was 10%, 13%, 16%, and 19% for the silica sand and field sand, and 54%, 59%, 64%, and 67% for the field clay. After the soil-ring structure was frozen at the target temperature for more than 24 h, the punch head and bottom ring support were assembled with soil-ring

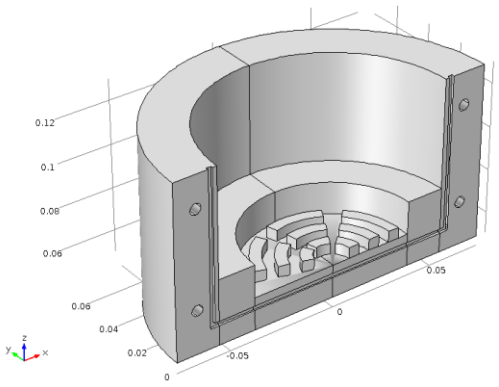

(a) Back mold unit

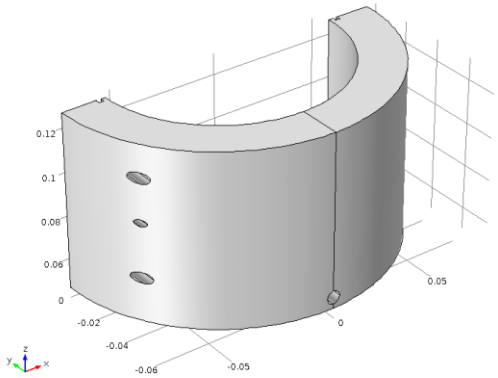

(b) Front mold unit

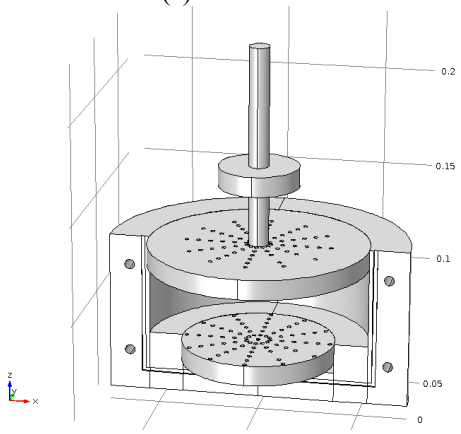

(c) Back mold unit with porous plates

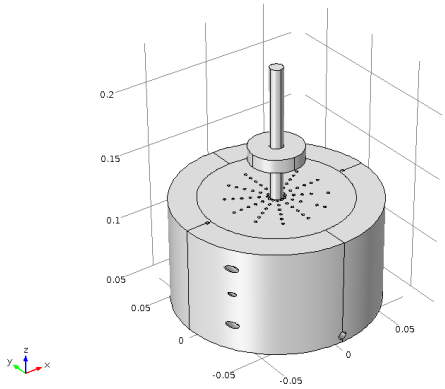

(d) Assembly of the mold

(e) Overview of the preparation mold

(f) Overview of the preparation mold with a weight

Fig. 6 Soil-ring structure preparation mold

structures, and then the punch shear test was conducted. The compressive force from the compressive apparatus was applied to the punch head, and the upward velocity of the pedestal was 1 mm/min.

3. Experimental results

After the punch test, the frozen soil specimen was dismantled from the ring, as illustrated in Fig. 7. Because there is no crack or damage on the frozen soil specimen, it can be seen that the compressive force was delivered well to the sheared surface.

As shown in Figs. 8 and 9, the shear stress-displacement curves from the punch shear test showed a strain-softening behavior, similar to the typical shape of the stress-displacement curve from the direct shear test. Before the shear stress reached the maximum value, the adfreeze bonding due to the ice was intact such that the interface firmly withstood the shear stress. However, the shear stress drastically decreased after reaching the maximum shear stress, which means that the adfreeze bonding was broken. Then, the interface between the soil and ring structure resisted the residual shear strength. As the target temperature decreased and the initial water content increased, the strain-softening behavior became more

Fig. 7 Field clay-stainless steel ring structure after test

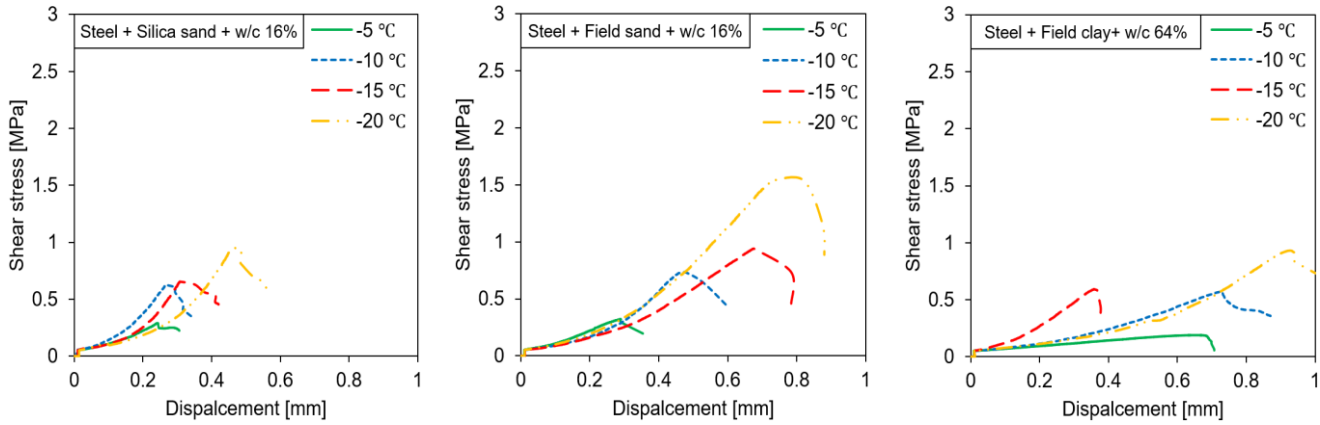

(a) Silica sand (b) Field sand (c) Field clay

Fig. 8 Shear stress−displacement curves with steel ring structure at constant water content

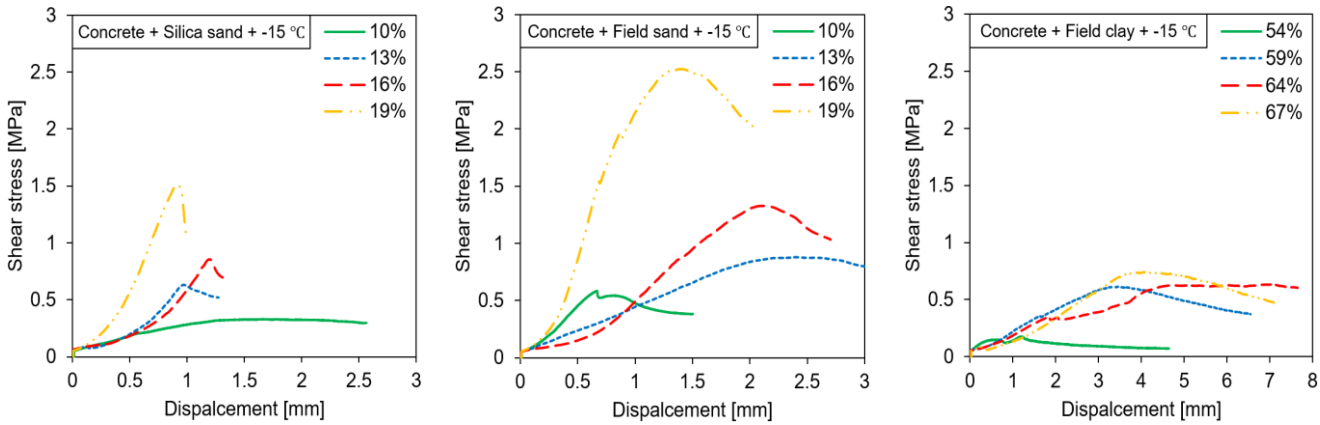

(a) Silica sand (b) Field sand (c) Field clay

Fig. 9 Shear stress−displacement curves with concrete ring structure at -15°C

distinct. The displacement corresponding to the maximum shear stress, at which the soil specimen and the ring structure separated, tended to be different depending on the soil specimens and the ring structure materials. The silica sand showed the shortest displacement until reaching the maximum shear stress, followed by field sand and field clay in order. These segregation points occurred within 1 mm with the steel ring structure, whereas most of the soil specimens detached from the concrete ring structure more than 1 mm, up to 7 mm. However, there is no clear trend in the slope before reaching the peak or residual strength.

Fig. 10 depicts the variation in the adfreezing strength for frozen soil and steel ring structure with the temperature at constant water content (i.e., 16% for sands and 64% for field clay. It can be seen from Fig. 10 that the adfreezing strength tended to increase with a decrease in temperature.

The other result for the influence of water content illustrated in Fig. 11 indicates that the adfreezing strength

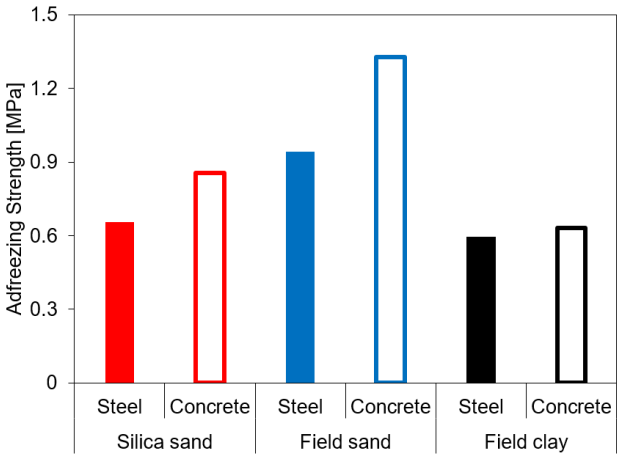

Fig. 12 Comparison of adfreezing strength depending on the ring structure material

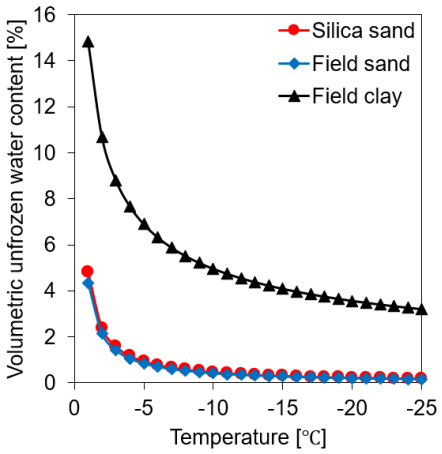

Fig. 13 Volumetric unfrozen water content versus temperature below 0℃ for three soil specimens

between the soil and concrete ring structure increases with increasing water content at -15°C. Even though the field clay had the highest water content compared with the other sands, the field sand showed the largest adfreezing strength, followed by the silica sand and field clay under the same temperature and ring structure. The rate of increase of the adfreezing strength is also in the order of field sand, silica sand, and field clay. For instance, the slopes of adfreezing strength over temperature and water content of silica sand and field sand were steeper than those of field clay.

The effect of the ring material on the adfreezing strength can be considered from the experimental results. Fig. 12 displays the adfreezing strength, depending on the ring structure material under the same conditions, which are 16% of water content and -15°C for two sands, and 64% of water content and -15°C for field clay. The adfreezing strength was greater in the concrete ring structure than in the stainless steel ring for all the soil specimens.

4. Discussions

4.1 Effect of unfrozen water content

Because the primary mechanism of adfreezing is the adhesive strength of ice, it is evident that the adfreezing strength is proportional to the ice content. For a given initial water content in the soil before freezing, the ice content should decrease if the unfrozen water content increases. Moreover, the unfrozen water content can lubricate to reduce the friction resistance of soil particles. Hence, the adfreezing strength has an inverse relationship with the unfrozen water content. As such, the exploration of unfrozen water content would help in analyzing the experimental results.

There are empirical and theoretical approaches for calculating the unfrozen water content. Although theoretical approaches that require many parameters are more accurate than some empirical approaches, empirical approaches have been frequently used in practical applications because of their usability. This section follows the method of Aukenthaler (2016), which estimated the water content from several empirical models.

Anderson and Tice (1972) proposed an empirical formulation using Eq. (2) as a power function for calculating the unfrozen water content W_{unf}, defined as the percentage of water weight by weight of dry soil.

$$W_{unf} = \alpha(-T)^{\beta} \tag{2}$$

where α and β are empirical fitting parameters as functions of the specific surface area, SSA, calculated from Eqs. (3) and (4), respectively, and T denotes the temperature.

$$\alpha = exp[0.5519ln(SSA) + 0.2618] \tag{3}$$

$$\beta = -exp[-0.2640ln(SSA) + 0.3711] \tag{4}$$

To obtain SSA, another empirical model based on the geometric mean of soil particle diameter (d_g) was determined by non-linear regression analysis as follows (Sepaskhah *et al.* 2010)

$$SSA = 3.89d_g^{-0.905} \tag{5}$$

The particle size distribution of soil has often been assumed to have a lognormal distribution. Based on this assumption, the geometric mean of the soil particle diameter was approximated by Eq. (6), according to the USDA system (Shirazi and Boersma 1984).

$$d_g = exp\left[0.01\left(f_{sand}ln(D_{sand}) + f_{silt}ln(D_{silt}) + f_{clay}ln(D_{clay})\right)\right] \tag{6}$$

where f_{sand}, f_{silt}, and f_{clay} are the mass percentages of sand, silt, and clay, respectively, and D_{sand}, D_{silt}, and D_{clay} are the upper limits of particle size for sand, silt, and clay, respectively (D_{sand} = (2 + 0.05)/2 = 1.025 mm, D_{silt} = (0.05 + 0.002)/2 = 0.026 mm, D_{clay} = (0.002 + 0)/2 = 0.001 mm).

After the specific surface area was determined from the particle size distribution curves in Fig. 3, the volumetric

unfrozen water content with temperature for the given soil specimens was obtained and is shown in Fig. 13. The unfrozen water content of all soil types decreased rapidly to approximately -5°C and then slowly decreased with decreasing freezing temperature. Therefore, the lower temperature would have enhanced the pore water to ice and enhanced the adfreezing strength, as shown in Fig. 10. Field clay with a larger mass fraction of finer particles showed higher unfrozen water content than the other soil specimens. This result explains why field clay had the lowest value of adfreezing strength independent of the ring structure material, even if it had a higher initial water content.

In the case of sands, the adfreezing strength considerably increased as the initial water content increased, because the two types of sand had almost zero unfrozen water content at -15°C, which means that most of the increased pore water caused increased ice content. Meanwhile, because the field clay still has some amount of unfrozen water content, the adfreezing strength slightly increased with an increase in the initial water content.

Although there is no significant difference in the unfrozen water content between silica sand and field sand, the adfreezing strength of field sand is much greater than that of silica sand. This means that the adfreezing strength was affected not only by the unfrozen water content but also other additional factors. In the case of coarse-grained soil, particle grading and roughness of the structure are considered important factors affecting the soil-structure interface behavior (Donna *et al.* 2015). The effects of these factors will be discussed in the next section.

4.2 Effect of ring structure's roughness

The surface roughness considering soil particle size can be described through the normalized roughness of the structure, R_n, proposed by Uesugi and Kishida (1986) in Eq. (7). They found that the interface resistance linearly increased with the normalized roughness until the critical roughness, where the interfacial resistance no longer increased and had a constant value.

$$R_n = \frac{R_{max}}{D_{50}} \tag{7}$$

where R_{max} is the maximum groove depth of the uneven surface, and D_{50} is the medium diameter of the soil particle.

When the maximum groove depth was identical for the same material, the normalized roughness was determined by the medium diameter of the soil particles. The medium diameter was around 1 mm for silica sand and 0.22 mm for field sand. Thus, the normalized roughness of the field sand was approximately 4.54 times larger than that of the silica sand with the same ring material, and the adfreezing strength with the field sand was larger than that of the silica sand.

Because concrete was rougher than stainless steel with bare eyes as shown in Fig. 4 (i.e., the maximum groove depth of concrete was larger than that of stainless steel), the normalized roughness of concrete was larger than that of stainless steel with the same soil specimen, and the adfreezing strengths with the concrete ring had larger values, as shown in Fig. 12. Although there can be the same conclusion for the field clay, the particle of field clay is too small. Hence, the difference is not that apparent.

4.3 Effect of sample dimension

In this study, a standard dimension of the soil specimen and ring structure cannot be suggested because there is no proposed sample size as a criterion for the punch shear test, even in rock mechanics. However, the adfreezing strength between ice and materials is dependent on the sample dimension (Nakazawa *et al.* 1988, Terashima 1997), and the experimental results from the proposed punch shear test for adfreezing strength could also differ depending on the sample dimensions. Thus, it is necessary to explore the influence of the sample dimensions in further research.

5. Conclusions

Multiple laboratory experiments have been carried out to determine the adfreezing strength using a direct shear test, which is simple and can reflect a confined condition. In practice, however, it is sometimes necessary to obtain unconfined adfreezing strength assuming a critical situation, and the direct shear test requires specific models to predict that strength. In this study, the punch shear test, which can directly measure the shear strength of rock with zero confinement, is suggested to evaluate the adfreezing strength between frozen soil and structure with a suitable specimen preparation method. The punch shear test system consisted of a punch head, soil-ring structure, and bottom ring support, and the adfreezing strength was calculated under different conditions: soil types, materials of the ring structure, water content, and temperature. The test results were analyzed and discussed, and the conclusions are summarized as follows.

- The strain-softening behavior is shown in the shear stress-displacement curves. After the interface between the soil specimen and ring structure strongly resisted until the shear stress reached the peak stress, the ice bonding was broken, and the interface stood the load with residual strength.
- The adfreezing strength increased with decreasing temperature. The unfrozen water content obtained by the empirical equations was reduced (i.e., the ice content increased at a constant initial water content) at a lower temperature.
- The adfreezing strength increased as the initial water content increased. For the sands, the unfrozen water content was very small at the target temperatures. Therefore, the high initial water content directly increased the ice content and strengthened the adfreezing bonding. In contrast, because relatively sizable unfrozen water remained for the field clay, the increasing rate of adfreezing strength with the initial water content diminished.
- The particle size distribution of the soil impacted the behavior of the frozen soil-structure interface both

directly and indirectly. The distribution of grain size can be used to calculate the specific surface area affecting unfrozen water content and is an influential property characterizing granular soils. Field clay with small particles had the largest unfrozen water content and showed lower adfreezing strength than the others. The field sand with a larger normalized roughness obtained from D_{50} than silica sand showed the largest adfreezing strength.

- The ring material, which had a rougher surface, brought about larger particle friction, so that the frozen soil with a concrete ring structure showed a larger adfreezing strength than that with a stainless steel ring structure.
- The proper dimensions of the sample were not considered in this study. However, because the sample size could affect the adfreezing strength, further research is needed to estimate the effect of sample dimensions through additional experiments and numerical analyses.

Acknowledgments

This research was supported by the National Research Foundation of Korea (NRF) grants funded by the Korea government (2019R1A2C2086647 and 2020R1A6A1A030 45059).

References

Anderson, D.M. and Tice, A.R. (1972), "Predicting unfrozen water contents in frozen soils from surface area measurements", *Highway Res. Record*, **393**(2), 12-18. https://doi.org/10.1016/0022-4898(73)90017-7.

Arenson, L.U., Johansen, M.M. and Springman, S.M. (2004), "Effects of volumetric ice content and strain rate on shear strength under triaxial conditions for frozen soil samples", *Permafrost Periglacial Processes*, **15**(3), 261-271. https://doi.org/10.1002/ppp.498.

Aukenthaler, M. (2016), "The Frozen & Unfrozen Barcelona Basic Model", M.S. Dissertation, Delft University of Technology.

Burt, T.P. and Williams, P.J. (1976), "Hydraulic conductivity in frozen soils", *Earth Surf. Processes*, **1**(4), 349-360. https://doi.org/10.1002/esp.3290010404.

Choi, C. (2011), "A study on the effect of pile surface roughness on adfreeze bond strength", *J. Korean GEO Environ. Soc.*, **12**(12), 79-88.

Di Donna, A., Ferrari, A. and Laloui, L. (2016), "Experimental investigations of the soil–concrete interface: physical mechanisms, cyclic mobilization, and behaviour at different temperatures", *Can. Geotech. J.*, **53**(4), 659-672. https://doi.org/10.1139/cgj-2015-0294@cgj-wgge.issue01.

He, P., Mu, Y., Yang, Z., Ma, W., Dong, J. and Huang, Y. (2020), "Freeze-thaw cycling impact on the shear behavior of frozen soil-concrete interface", *Cold Regions Sci. Tech.*, **173**, 103024. https://doi.org/10.1016/j.coldregions.2020.103024.

Jaeger, C. (1979), *Rock Mechanics and Engineering*, (2nd Edition), Cambridge University Press.

Jin, H., Lee, J., Zhuang, L. and Byu, B.H. (2020), "Laboratory investigation of unconfined compression behavior of ice and frozen soil mixtures", *Geomech. Eng.*, **22**(3), 219-226. https://doi.org/10.12989/gae.2020.22.3.219.

Ko, S.G. and Choi, C.H. (2011), "Experimental study on adfreeze bond strength between frozen sand and aluminium with varying freezing temperature and vertical confining pressure", *J. Korean Geotech. Soc.*, **27**(9), 67-76. https://doi.org/10.7843/kgs.2011.27.9.067.

Ladanyi, B. (1995), "Frozen soil—structure interfaces", *Studies Appl. Mech.*, **42**, 3-33. https://doi.org/10.1016/S0922-5382(06)80004-8.

Lee, J., Kim, Y. and Choi, C. (2013), "A study for adfreeze bond strength developed between weathered granite soils and aluminum plate", *J. Korean Geoenviron. Soc.*, **14**(12), 23-30. https://doi.org/10.14481/jkges.2013.14.12.023.

Li, L.R., Deng, J.H., Liu, J.F., Zheng, J., Chen, T. and Deng, C.F. (2017), "A new understanding of punch-through shear testing", *Géotechnique Lett.*, **7**(2), 129-135. https://doi.org/10.1680/jgele.16.00123.

Liu, J., Lv, P., Cui, Y. and Liu, J. (2014), "Experimental study on direct shear behavior of frozen soil–concrete interface", *Cold Regions Sci. Technol.*, **104**, 1-6. https://doi.org/10.1016/j.coldregions.2014.04.007.

Nakazawa, N., Saeki, H., Ono, T., Takeuchi, T. and Kanie, S. (1988), "Ice forces due to changes in water level and adfreeze bond strength between sea ice and various materials", *J. Offshore Mech. Arct. Eng.*, **110**(1), 74-80. https://doi.org/10.1115/1.3257127.

Parameswaran, V.R. (1978), "Adfreezing strength of frozen sand to model piles", *Can. Geotech. J.*, **15**(4), 494-500. https://doi.org/10.1139/t78-053.

Peng-Fei, H.E., Yan-Hu, M.U., Wei, M.A., Huang, Y.T. and Jian-Hua, D.O.N.G. (2021), "Testing and modeling of frozen clay–concrete interface behavior based on large-scale shear tests", *Adv. Climate Change Res.*, **12**(1), 83-94. https://doi.org/10.1016/j.accre.2020.09.010.

Quanbin, S., Ping, Y. and Guoliang, W. (2018), "Experimental research on adfreezing strengthsat the interface between frozen fine sand and structures", *Scientia Iranica*, **25**(2), 663-674. https://doi.org/10.24200/SCI.2017.20005.

Sayles, F.H. and Carbee, D.L. (1981), "Strength of frozen silt as a function of ice content and dry unit weight", *Eng. Geol.*, **18**(1-4), 55-66. https://doi.org/10.1016/0013-7952(81)90046-6.

Sepaskhah, A.R., Tabarzad, A. and Fooladmand, H.R. (2010), "Physical and empirical models for estimation of specific surface area of soils", *Arch. Agronomy Soil Sci.*, **56**(3), 325-335. https://doi.org/10.1080/03650340903099676.

Shirazi, M.A. and Boersma, L. (1984), "A unifying quantitative analysis of soil texture", *Soil Sci. Soc. Am. J.*, **48**(1), 142-147. https://doi.org/10.2136/sssaj1984.03615995004800010026x.

Tang, L., Du, Y., Liu, L., Jin, L., Yang, L. and Li, G. (2020), "Effect mechanism of unfrozen water on the frozen soil-structure interface during the freezing-thawing process", *Geomech. Eng.*, **22**(3), 245-254. https://doi.org/10.12989/gae.2020.22.3.245.

Terashima, T. (1997), "Comparative experiments on various adfreeze bond strength tests between ice and materials", *WIT T. Eng. Sci.*, **14**, 207-216. https://doi.org/10.2495/CON970211.

Thomas, H.R., Cleall, P., Li, Y.C., Harris, C. and Kern-Luetschg, M. (2009), "Modelling of cryogenic processes in permafrost and seasonally frozen soils", *Geotechnique*, **59**(3), 173-184. https://doi.org/10.1680/geot.2009.59.3.173.

Uesugi, M. and Kishida, H. (1986), "Frictional resistance at yield between dry sand and mild steel", *Soil. Found.*, **26**(4), 139-149. https://doi.org/10.3208/sandf1972.26.4_139.

Wang, D., Wang, T., Xu, D. and Zhou, G. (2020), "Estimation of spatial autocorrelation variations of uncertain geotechnical properties for the frozen ground", *Geomech. Eng.*, **22**(4), 339-348. https://doi.org/10.12989/gae.2020.22.4.339.

Wang, S., Wang, Q., Qi, J. and Liu, F. (2018), "Experimental study on freezing point of saline soft clay after freeze-thaw cycling", *Geomech. Eng.*, **15**(4), 997-1004. https://doi.org/10.12989/gae.2018.15.4.997.

Wang, T.L., Wang, H.H., Hu, T.F. and Song, H.F. (2019),

"Experimental study on the mechanical properties of soil-structure interface under frozen conditions using an improved roughness algorithm", *Cold Regions Sci. Tech.*, **158**, 62-68. https://doi.org/10.1016/j.coldregions.2018.10.015.

Wang, T., Zhou, G., Wang. J. and Wang, D. (2020), "Impact of spatial variability of geotechnical properties on uncertain settlement of frozen soil foundation around an oil pipeline", *Geomech. Eng.*, **20**(1), 19-28. https://doi.org/10.12989/gae.2020.20.1.019.

Weaver, J.S. and Morgenstern, N.R. (1981), "Pile design in permafrost", *Can. Geotech. J.*, **18**(3), 357-370. https://doi.org/10.1139/t81-043.

Wu, H., Kemeny, J. and Wu, S. (2017), "Experimental and numerical investigation of the punch-through shear test for mode II fracture toughness determination in rock", *Eng. Fract. Mech.*, **184**, 59-74. https://doi.org/10.1016/j.engfracmech.2017.08.006.

Xu, Y., Yao, W., Xia, K. and Ghaffari, H.O. (2019), "Experimental study of the dynamic shear response of rocks using a modified punch shear method", *Rock Mech. Rock Eng.*, **52**(8), 2523-2534. https://doi.org/10.1007/s00603-019-1744-x.

Zhang, Y., Cheng, Z. and Lv, H. (2019), "Study on failure and subsidence law of frozen soil layer in coal mine influenced by physical conditions", *Geomech. Eng.*, **18**(1), 97-109. https://doi.org/10.12989/gae.2019.18.1.097.

Zhu, T. and Li, Y. (2021), "Impacts of Disk Rock Sample Geometric Dimensions on Shear Fracture Behavior in a Punch Shear Test", *Comput. Model. Eng. Sci.*, **126**(2), 455-475. https://doi.org/10.32604/cmes.2021.014284.

Zhou, Z., Yang, H., Xing, K. and Gao, W. (2018), "Prediction models of the shear modulus of normal or frozen soil-rock mixtures", *Geomech. Eng.*, **15**(2), 783-791. https://doi.org/10.12989/gae.2018.15.2.783.